# Solidification of a main-chain liquid-crystal polymer: Effects of electric fields, surfaces and mesophase ageing

**P. G. Martin and S. I. Stupp**
*Department of Materials Science and Engineering, University of Illinois at Urbana–Champaign, Urbana, IL 61801, USA*
*(Received 11 February 1986; revised 14 August 1986; accepted 2 October 1986)*

Solid films of the liquid-crystal polycondensate of 80 mol% *p*-acetoxybenzoic acid and 20 mol% poly(ethylene terephthalate) were probed by exposures to controlled surfaces and electric fields and analysed by differential scanning calorimetry and X-ray diffraction. Films can develop some preferred backbone orientation after isothermal ageing of the mesophase and resolidification as a result of surface topography on confining walls. Mesophase ageing also results in solid films with greater structural order. Preferred backbone orientation is enhanced when solid films are heated to the liquid-crystalline state in an electric field and then resolidified. This is thought to result from the coupled effect of a pre-existing molecular field and dielectric alignment of the mesogenic chains. Interchain dipolar coupling and a biaxial nematic structure should be considered further as possible structural elements in these polymers.

**(Keywords: liquid-crystal polymer; mesophase; surface; electric field; mesophase ageing)**

## INTRODUCTION

Scientific and technological interest in macromolecular liquid crystals has grown considerably over the past few years. The scientific issues of interest in liquid-crystal polymers and their solids are quite numerous and it is clear that simple extrapolations from the widely studied monomeric systems are not always possible. Important questions include the nature of their submicroscopic structure, the factors that control their high-order parameters, the dynamics of main-chain systems in external fields, crystallization and the nature of local molecular motions. Technological interest so far is based on their well known but not fully realized potential as materials with superior mechanical and thermal properties. Over the past few years our group has been exploring the potential of liquid-crystal polymers as electroactive materials. This interest includes the use of these macromolecules to form highly ordered and electrically polar microstructures. Such materials could have useful properties, such as piezo- or pyroelectricity, non-linear optical or electro-optical behaviour, anisotropic conductivity and others. There are interesting examples in the literature on the use of liquid-crystal polymers as substrates for information storage[1] and the development of photoconductors[2,3].

A theoretical understanding of liquid crystallinity in polymers was first offered by the work of Flory[4–6]. The common structural feature of mesophase-forming polymers is the high aspect ratio and rigid conformation of the chains. Repulsive forces among the rigid molecules are viewed as the main driving force for their organization into liquid crystals. This concept is a central issue in the original theoretical work by Flory. The contribution of attractive and anisotropic intermolecular forces to the formation and stability of macromolecular liquid-crystalline phases is one of the many aspects poorly understood at the present time. Another important and related question is the role of intermolecular bonding in the response of liquid-crystal polymers to external fields (mechanical, surface, electrical, magnetic). In the case of electric and magnetic fields, this response could be governed to a significant degree by cooperative phenomena involving electric or magnetic moments which couple due to the polymeric nature of the mesophase. Given the long relaxation times of polymers and the cooperativity of mesophases, the vitrification or crystallization of liquid-crystalline polymers under the influence of electric or magnetic forces could also produce solid polar phases and their characteristic properties.

The interaction of electrical forces with liquid crystals is known to produce a variety of effects. The so-called Freedericksz transitions in macroscopically aligned mesophases are well known phenomena for liquid crystals of low molar mass. The dielectric anisotropy and cooperativity of molecules in the aligned mesophase leads to reorientation in an external field as illustrated in *Figure 1*. Molecules near the surface are pinned in their original preferred orientation due to surface forces and therefore only bulk regions are aligned in the field. Threshold voltages $V_{th}$ have been calculated assuming that reorientation occurs when the electric energy of deformation equals the dielectric energy[7]. For a system with negative dielectric anisotropy ($\varepsilon_{\parallel} < \varepsilon_{\perp}$), one may express the threshold voltage $V_{th}$ for electric reorientation:

$$V_{th}^2 = \pi^2 \frac{K_{33}}{(\varepsilon_{\perp} - \varepsilon_{\parallel})\varepsilon_0} \quad (1)$$

0032-3861/87/060897-10$03.00

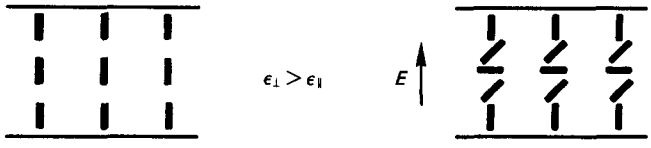


**Figure 1** Schematic representation of the Freedericksz transition in a liquid-crystalline monodomain

where $K_{33}$ is the bend elastic modulus and $\varepsilon_0$ is the permittivity of free space. Experiments based on the physical concept described above with high-melting-point and high-molecular-weight polymeric liquid crystals are not easily done, given their slow response to external fields. However, the general principle should apply to such polymers and it is helpful in the interpretation of some of our results.

In the context of electric field interactions, most of the previous work has involved low-molecular-weight liquid crystals[8-13], and much less is known about polymer liquid crystals. The polymeric systems studied so far include side-chain[14-17] as well as main-chain[18-24] liquid crystals. Side-chain systems have been found to have an orientational response time to electric fields which is comparable to that of low-molecular-weight liquid crystals. This is expected on the basis that mesogenic units in these systems are attached via flexible spacers to a polymeric backbone. On the other hand, the general response is known to be very sluggish in main-chain systems[18,19]. In general, most previous studies have focused on the behaviour of materials responding to an external electric field while in the mesophase. Our work has focused on the solidification of a main-chain liquid-crystalline copolyester while exposed to an electric field or after the mesophase is thermally aged. The polymer studied was the polycondensate of 80 mol% *p*-acetoxybenzoic acid and 20 mol% poly(ethylene terephthalate), and we have used solidified samples for experimental characterization. The synthetic reaction was first reported by Jackson and Kuhfuss[25]. X-ray diffraction and differential scanning calorimetry were the main techniques used in the investigation.

## EXPERIMENTAL

The copolymer utilized in this study was supplied to us in the form of extruded pellets by Tennessee Eastman in Kingsport, Tennessee. Three types of experimental films were prepared by heat pressing. In one type of film (type A) the pellets were aligned with the extrusion direction perpendicular to the film surface prior to heat pressing. The second type of film was prepared with pellets placed with the extrusion direction parallel to the film surface (type B), and the third with random orientation of pellets (type C) (see *Figure 2*). The pellets were carefully placed in a specially designed cell that applies a uniform thermal treatment to 36 samples during a given pressing. The cell consists of several plates surrounded by a K-20 refractory brick housing coated with high-temperature RTV to prevent dust from contaminating the samples. Samples are pressed between 0.05 mm thick Teflon sheets, which act as a mould release agent in the centre of the cell. Shim stock plates provide a smooth surface for pressing with the remainder of the plates providing heat-conducting channels. Before placing the mould in the press, the platens were heated to 300°C. The mould was allowed to equilibrate at the pressing temperature. Then a pressure of 1250 psi (8.62 MPa) was applied and the platen heaters turned off immediately. Pressure was maintained during the subsequent cooling from 300°C to room temperature by natural convection and radiation to the atmosphere (cooling took 7 h). Films A and B were pressed to a thickness of 350 $\mu$m, and films C to a thickness of 850 $\mu$m.

Pressed films were melted for mesophase ageing and exposure to electric fields in a thermally controlled cell shown schematically in *Figure 3*. The upper electrode was disc-shaped and the lower electrode was cup-shaped in order to contain the polymeric fluid. Both electrodes were gold-plated and covered with aluminium foil to facilitate removal of the specimens after the various treatments. The heater surrounding the electrode cell was connected to an Oyo Denshi type UZ-2140 thermal controller device whereas the electrode cell was connected to a Yokogawa type 2141 high-voltage supply capable of

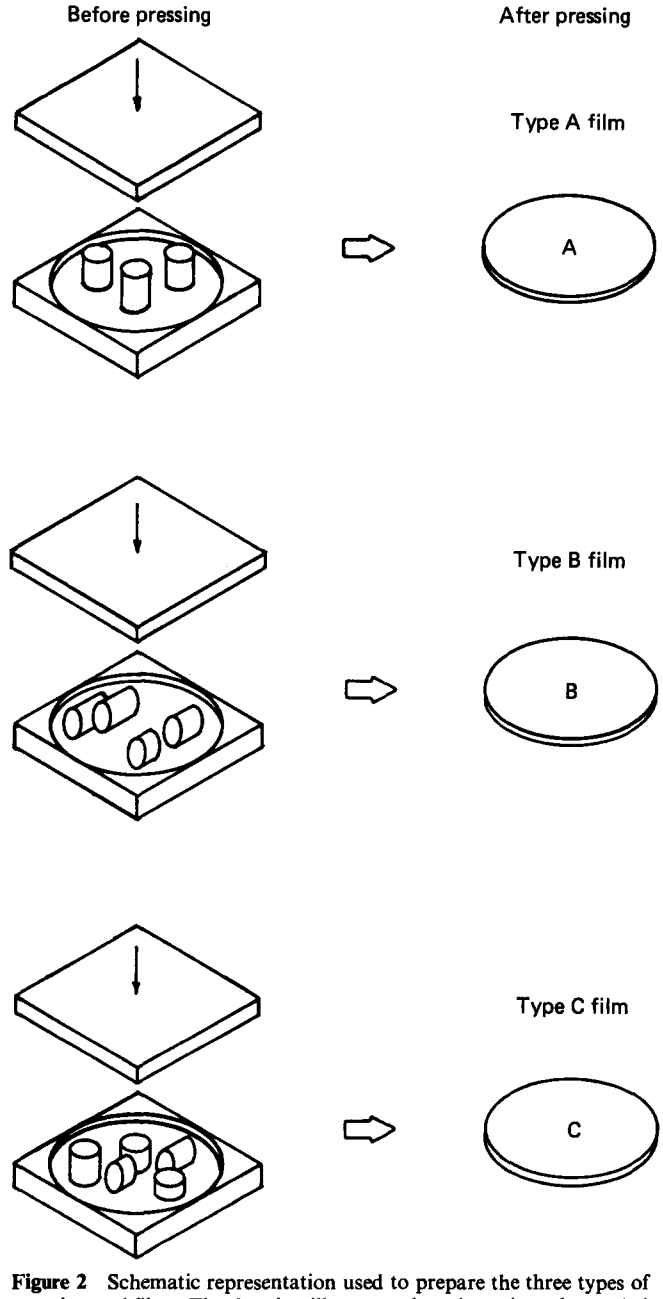


**Figure 2** Schematic representation used to prepare the three types of experimental films. The drawing illustrates the orientation of extruded copolymer pellets prior to heat pressing

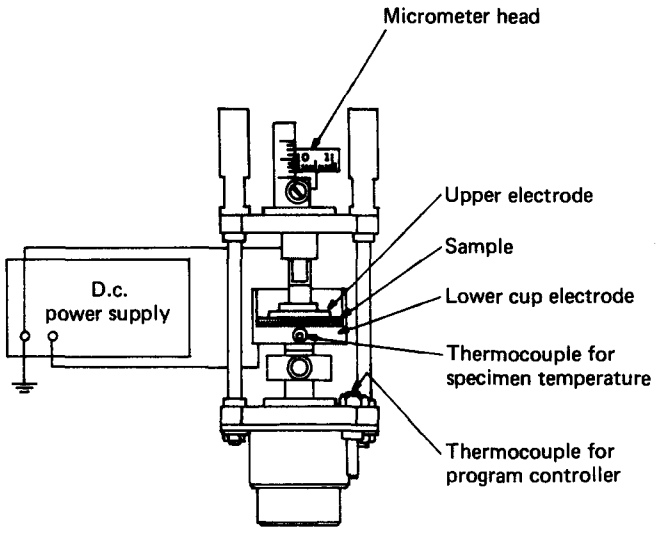


**Figure 3** Schematic drawing of the cell used to expose the mesophase to an electric field and thermal ageing

maintaining a constant potential. Current flowing through the samples was monitored at all times yielding resistivities of the order of $10^{11}\,\Omega\,cm$ at 300°C (resistivities were even higher at lower temperatures). Prior to heating the cell was purged with nitrogen gas. A positive pressure (10 psi; 68.9 kPa) was maintained throughout the duration of the experiment to minimize chemical degradation of the specimens. A $2°C\,min^{-1}$ heating rate to a plateau temperature of $300\pm0.5$°C was used for all experiments. After thermal treatments and/or electric field exposures, all the specimens were allowed to cool by natural convection to room temperature. Cooling rates were reproducible as indicated by strip chart readings of thermocouple millivoltage as a function of time. The plateau temperature was always $300\pm0.5$°C, a temperature at which the solid films had transformed into birefringent liquids. This was verified in our laboratory by observation of a thin sample between cross-polars in the hot stage of an optical microscope. Samples were kept for either 15 min or 3 h at the plateau temperature, with or without an electric field. Electrically exposed samples were allowed to resolidify and cool to room temperature under the field. Electric fields were applied at room temperature to some samples and maintained throughout the thermal cycle. The resolidified films were characterized within a few days after the thermal or thermoelectric treatments.

Films were examined by means of flat-plate X-ray diffraction patterns, differential scanning calorimetry (d.s.c.) and X-ray diffractometer scans. Transmission flat-plate diffraction patterns were obtained with a Philips Electronics Instruments X-ray scattering source using Cu Kα radiation and instrument settings for voltage and current of 30 kV and 12 mA respectively. Diffraction patterns of type A and type B films were taken before and after the thermal or thermoelectric treatments with the 0.02 inch (0.5 mm) diameter collimated beam of X-rays passing through the same region of the experimental sample both times. Densitometer traces were obtained with a Baird model RC3 atomic microphotometer using a scanning speed of $17.6\,\mu m\,s^{-1}$. D.s.c. measurements were obtained with a DuPont 1090 thermal analyser using an interactive d.s.c. V2.0 data analysis program. Sample weights for d.s.c. analysis ranged from 5.0 mg to 10.0 mg, and all samples were examined within the temperature range of 40 to 370°C at a heating rate of $10°C\,min^{-1}$. A constant flow of nitrogen of $40\,cm^3\,min^{-1}$ was passed through the sample chamber throughout the d.s.c. experiment. X-ray scans were obtained with a Philips Norelco vertical scanning diffractometer with a graphite monochromator (Cu Kα radiation).

## RESULTS AND DISCUSSION

### *Mesophase ageing*

*Figure 4* shows a typical X-ray diffractometer scan of a thermally cycled type C film, aged in the liquid-crystalline phase for 15 min and resolidified. The scan shows a large scattering peak at $2\theta = 19.7°$ corresponding to a $d$ spacing of 4.50 Å, and a smaller peak at $2\theta = 23.7°$ corresponding to a $d$ spacing of 3.75 Å. These peaks correspond to $d$ spacings reported by Economy *et al.*[26] for poly(*p*-hydroxybenzoic acid) (PHB), the homopolymer resulting from the condensation of *p*-acetoxybenzoic acid. The simplest conclusion from the diffractometer scan is that PHB blocks are present in the copolymer and segregate to form PHB crystals in the solid film. However, we point out that the nature of the chemical sequence, the copolymer vs. blend character and the phase structure of this family of liquid-crystalline polyesters are still controversial issues which have not been resolved[25,27-30]. In the context of these uncertainties, two facts are important to the work reported here. One is that the material studied begins to melt into a birefringent fluid just below 300°C (this was verified in our laboratory by optical microscopy between cross-polars). However, we suspect that this fluid mesophase contains solid material at 300°C. The existence of higher-melting material is evidenced by d.s.c. data (discussed later). Thus, the fluid mesophase at 300°C could be thought of as a 'filled liquid crystal' (solid material dispersed in the anisotropic liquid). The other important fact is that the fluid solidifies into a material containing ordered regions. The exact nature of these ordered regions (chemical defects, conformational disorder, intermolecular correlations) is unknown to us. For this reason, in the discussion of our work we prefer the use of the word 'solidification' rather than 'crystallization'. When the word 'crystallization' (or 'crystallinity') is used, it is done with full apprecitation of the fact that the detailed solid-state structure in these materials is as yet unknown.

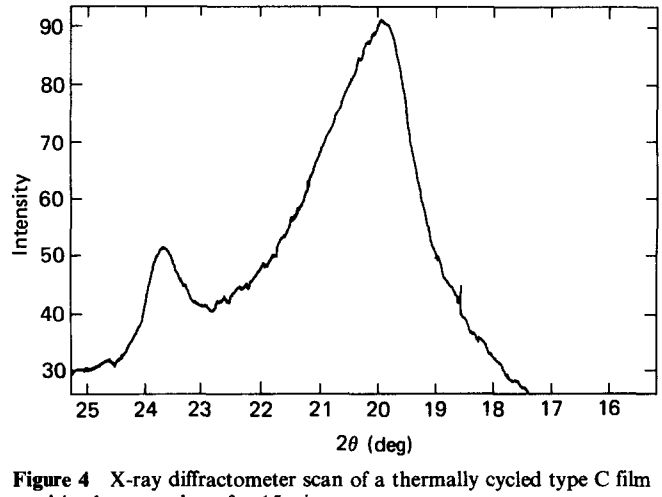


**Figure 4** X-ray diffractometer scan of a thermally cycled type C film aged in the mesophase for 15 min

We estimated a relative degree of crystallinity in extruded pellets and different types of films using X-ray diffractometer scans (see *Table 1*). An amorphous reference was defined by drawing a smooth curve through the shoulders of peaks from an X-ray scan of an extruded pellet over the range from $2\theta = 10°$ to 34°. The curve was defined in this way since we were unable to quench this material into an amorphous state for a reference scan. A relative degree of crystallinity for all other samples was determined by scaling the amorphous curve to each scan as outlined by Challa *et al.*[31] An important result revealed by the table is the fact that all film samples have a significantly higher percentage crystallinity relative to the extruded pellet from which samples were prepared. Average enthalpy values, $\Delta H$, obtained by integration of the melting peak in the region of 300°C (see *Figure 5*), are listed in *Table 2*. The larger $\Delta H$ in pressed films is consistent with the observed differences in percentage crystallinity measured from X-ray scans. The lower crystallinity in extruded pellets could be the result of a fast cooling rate and/or slow crystallization in the oriented nematic.

Data in *Table 1* also suggest that ageing time in the liquid-crystalline phase slightly raises the final degree of crystallinity in the films. A mechanism involved in the enhanced crystallinity might be the gradual increase in axial registry among rigid chains during mesophase ageing. This increase in registry (intermolecular overlap of similar repeating units or phenyl groups) could be viewed as a gradual increase in the degree of smectic character in a nematic mesophase, which upon solidification raises the apparent 'crystallinity'. Another contributing mechanism would be that of crystallization-induced reaction in liquid-crystalline polyesters proposed by Lenz *et al.*[32] The mechanism involves transesterification reactions which occur when the mesophase is annealed. It was suggested that these reactions produce blocks of oxybenzoate units in the copolymer and consequently the formation of PHB crystals. The evidence for this suggestion includes the appearance of insoluble products when the mesophase is annealed. Generally speaking, the data suggest that chemical sequences or their intermolecular correlations are metastable and thus thermal history prior to solidification induces structural change. Our d.s.c. data on films resolidified after mesophase ageing reveal lower $\Delta H$ values after a thermal cycle for periods in the range of 15 to 30 min (see *Table 2*). Also, as shown in *Table 6*, the general trend is for mesophase ageing to shift the endotherm to higher temperatures. A possible interpretation of decreasing values of $\Delta H$ is the formation of infusible crystals. A feature common to all d.s.c. scans of thermally cycled films is a very broad endotherm suggesting broad distribution of order and sizes among the crystals.

**Table 1** Relative percentage crystallinity for various types of samples solidified from the liquid-crystalline state

| Sample | Ageing time in the mesophase (min) | Relative crystallinity (%) |
|---|---|---|
| Extruded pellet | 0 | 37 |
| Heat-pressed film (type C) | 0 | 61 |
| Thermally cycled type C film | 95 | 68 |
| Thermally cycled type A film | 15 | 63 |
| Thermally cycled type A film | 180 | 85 |
| Thermally cycled type B film | 15 | 60 |
| Thermally cycled type B film | 180 | 67 |

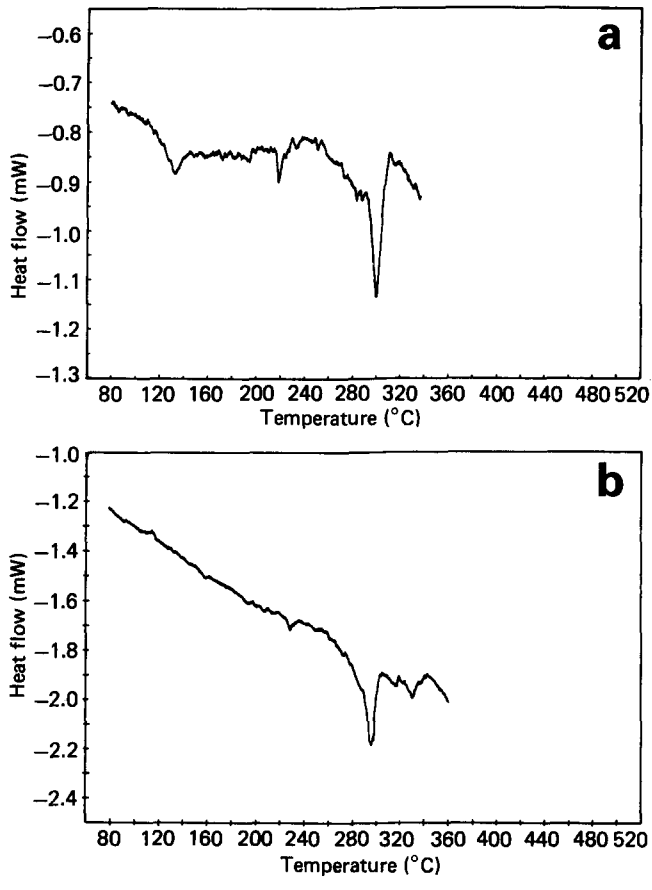


**Figure 5** D.s.c. scans of (a) extruded pellet and (b) heat-pressed film

**Table 2** Average enthalpy values as measured by d.s.c.

| Sample | $\Delta H$ (J g$^{-1}$)[a] |
|---|---|
| Extruded pellet | 2.44±0.28 |
| Heat-pressed film | 9.81±1.14 |
| Thermally cycled film, mesophase ageing in the range of 15–30 min | 6.85±1.70 |

[a] Value ± one standard deviation

Our initial work on films labelled as type C led us to the experimental protocol of preparaing type A and type B films (see *Figure 1*). The degree of orientation observed in films produced by heat pressing randomly arranged pellets was found to be a sensitive function of the location chosen for the X-ray beam path. The photographs in *Figure 6*, on the other hand, suggest that molecular orientation observed in melted and resolidified films originates in the uniaxial orientation present in extruded pellets before heat pressing. Extruded pellets should have a preferred molecular alignment along the extrusion direction. Therefore, one expects that type B films could have a preferred planar as well as uniaxial orientation of the chains. On the other hand, in type A films one expects a higher degree of chain orientation along the thickness of films. An important point is that orientation is retained in resolidified films after the original pellets are liquefied under pressure. Interestingly, significant molecular orientation can remain even in films resolidified a second time from a mesophase which was thermally aged for periods of 15 to 30 min.

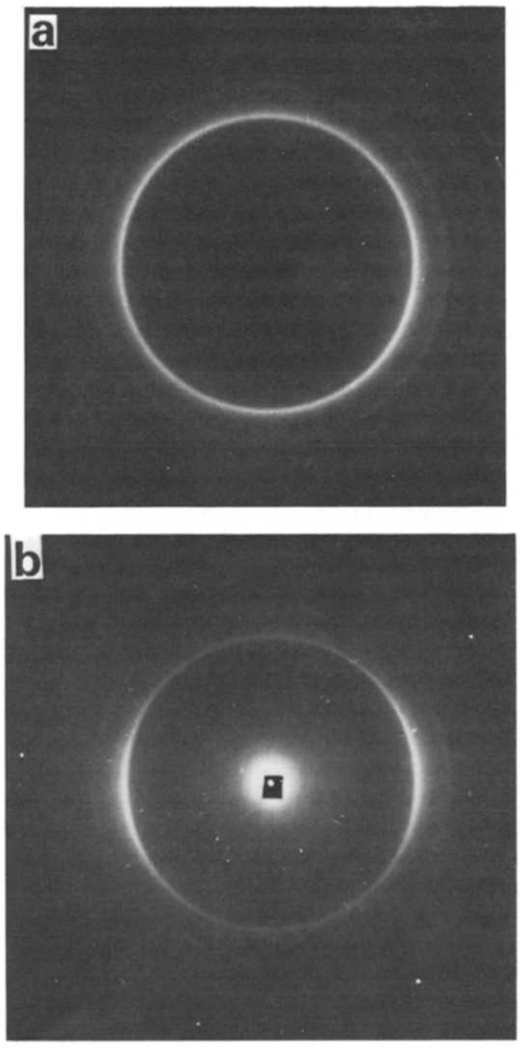


**Figure 6** Flat-plate diffraction photographs of a typical heat-pressed type A film (a) and of a typical heat-pressed type B film (b)

Using X-ray photographs, we analysed the degree of molecular orientation in films prepared with controlled alignment of the extruded pellets (types A and B). This was carried out using two different techniques and both involved analysis of the most intense Debye ring. This ring is associated with a scattering angle of $2\theta = 19.4°$, and based on a hexagonal crystal system proposed for PHB[26] it corresponds most likely to (1 0 4) planes with some contribution from (2 2 0) planes. In one technique we measured the angle between the lines passing through the centre of the photographs and the edges of the diffraction arcs (see *Figure 7*). In the second technique we radially scanned the Debye ring at 15° intervals with a densitometer, and measured the area under the curves in all 24 scans. In order to obtain relative degrees of orientation through a mathematical model, we calculated the ratio of the standard deviation to the mean of the 24 densitometer area measurements for each sample. This technique provides a more quantitative means of assessing orientational changes relative to arc angle measurements. As shown in the plot of *Figure 8*, a higher ratio implies a higher degree of orientation. The model and its calculations have been explained in the Appendix.

In analysing orientation for films of type A and B, we also controlled the region through which the X-ray beam passed before and after any thermal or electrical treatment. This was done by carefully marking all films in an attempt to minimize the location dependence effect observed in type C films. Thus, for each thermal or thermoelectric exposure of heat-pressed films we recorded an X-ray photograph termed 'initial' and one termed 'final' corresponding to the same film before and after thermal or thermoelectric treatment. *Tables 3* and *4* summarize initial and final values of the arc angle in type A and type B films. These tables also present data on the ratio of the standard deviation to the mean of densitometer area measurements ($\sigma/\bar{x}$ values). An important finding was a detectable level of orientation in resolidified type A and type B films even after the liquid-crystalline fluid was aged for periods of 3 h. Most of the solid films analysed had detectable orientation before mesophase ageing. However, specific regions in some type A films were seemingly unoriented and, interestingly, were found to develop some orientation after mesophase ageing and resolidification. Actual photographs showing this change are shown in *Figure 9*. We have considered two different phenomena in order to understand the enhanced orientation. One is that preferred orientation of the director in the original pressed film (in some cases hardly detectable) is preserved or enhanced by thermal ageing in the liquid-crystalline phase. This could occur through the preferential growth of some domains at the expense of others. Another possibility is that the enhanced orientation is associated with the nature of surfaces confining the mesophase. We investigated this particular aspect in some detail and results on the subject are discussed below.

*Surfaces*

The mesophase is first in contact with a Teflon surface during heat pressing and then with aluminium foil during mesophase ageing. We hypothesized that substrate topography could induce orientation since the director

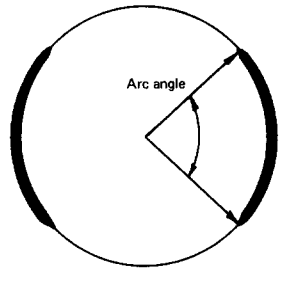


**Figure 7** Definition of arc angle

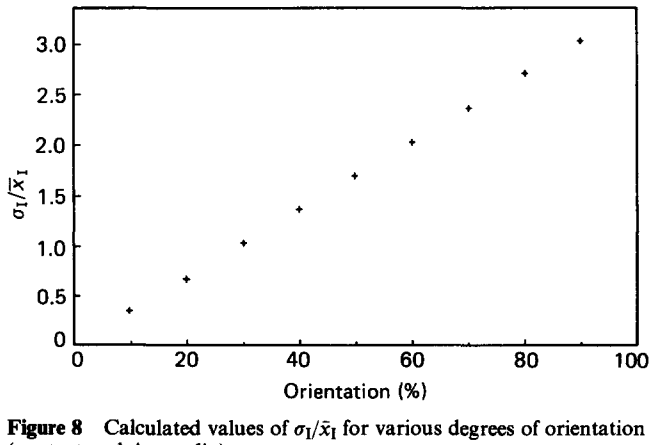


**Figure 8** Calculated values of $\sigma_I/\bar{x}_I$ for various degrees of orientation (see text and Appendix)

**Table 3** X-ray arc angles as a measure of molecular orientation in type A films prior to and after thermal or thermoelectric treatments

| Electric field[a] exposure | Time in mesophase (min) | Arc angle (deg) | | $\sigma_I/\bar{x}_I$ | |
|---|---|---|---|---|---|
| | | Initial | Final | Initial | Final |
| None | 15 | 180 | 180 | 0.520 | 0.422 |
| | 180 | 180 | 135 | 0.166 | 0.639 |
| *E* field applied in the liquid-crystalline state | 15 | 122 | 128 | 0.786 | 0.472 |
| | 180 | 115 | 99 | 0.563 | 0.583 |
| *E* field applied prior to solid-to-liquid crystal transition | 15 | 115 | 92 | 0.442 | 0.848 |
| | 180 | 180 | 116 | 0.459 | 0.467 |

[a] *E* field $\simeq 20000$ V cm$^{-1}$

**Table 4** Orientation in type B films, as measured by X-ray arc angles as a measure of molecular orientation in type B films prior to and after thermal or thermoelectric treatments

| Electric field[a] exposure | Time in mesophase (min) | Arc angle (deg) | |
|---|---|---|---|
| | | Initial | Final |
| None | 15 | 180 | 112 |
| | 180 | 77 | 88 |
| *E* field applied in the liquid-crystalline state | 15 | 88 | 88 |
| | 180 | 132 | 121 |
| *E* field applied prior to solid-to-liquid crystal transition | 15 | 75 | 77 |
| | 180 | 67 | 70 |

[a] *E* field $\simeq 20000$ V cm$^{-1}$

axis in liquid crystals is known to align along grooves on confining glass surfaces[33]. We examined by SEM the Teflon and aluminium surfaces which contact the mesophase and observed the presence of well defined grooves (see *Figure 10*). This observation led us to a whole series of experiments in which we not only controlled the location of X-ray analysis but also the relative alignment of grooves on the top and bottom Teflon or aluminium surfaces in contact with the material. We made films with parallel or perpendicular grooves on the top and bottom Teflon surfaces. We found no significant difference in orientation between the two types of samples. Interestingly, however, we discovered after several experiments that the longer time of contact with grooves on the aluminium surfaces does influence orientation in resolidified films. Based on our experiments, the enhanced orientation is sensitive to ageing temperature, pressure, initial state of orientation and cooling rate. We observed it after ageing temperatures in the range of 300 to 305°C but not below these temperatures. Also, cooling rates had to be of the order of 4°C min$^{-1}$, and pressure seemed to be important in cases where there was no detectable initial orientation. Our general observation was that orientation in films resolidified after mesophase ageing occurred when grooves on aluminium top and bottom surfaces were parallel. When grooves in top and bottom surfaces were positioned at 90° to each other, the flat-plate diffraction pattern does not reveal enhanced orientation. This may occur because the normal position of grooves in the two metal–polymer interfaces induces a gradual 'cholesteric' twist of director orientation through the film's thickness (see *Figure 11*). This surface-induced phenomenon occurs in low-molar-mass liquid crystals and can produce electro-optical effects when an external electric field biases the director's orientation[34]. Typical results from X-ray experiments on the effects of surfaces are shown in *Figure 12*.

*Electric fields*

Some experiments involved exposing the mesophase to an electric (*E*) field upon melting for a given period of time and then soldifying the liquid crystal under the influence of the field. In other experiments, the field was applied at room temperature while the sample was heated and melted. *Table 5* contains a summary of $\Delta H$ values for samples exposed to *E* fields under various conditions. Relative to thermal controls, $\Delta H$ values for the broad endotherm are higher in solid films solidified under the influence of *E* fields. This was found to be the case for fields in the range of 16 000 to 43 000 V cm$^{-1}$ (electrical breakdown occurred in most experiments involving fields in the region of 60 000 V cm$^{-1}$). The higher $\Delta H$ values in field-solidified samples are close to or slightly higher than those of heat-pressed films which were not exposed to thermal ageing. The endotherm also shifted to higher temperatures in field-solidified samples (see *Table 6*). We suggested earlier that the lower $\Delta H$ values in thermally

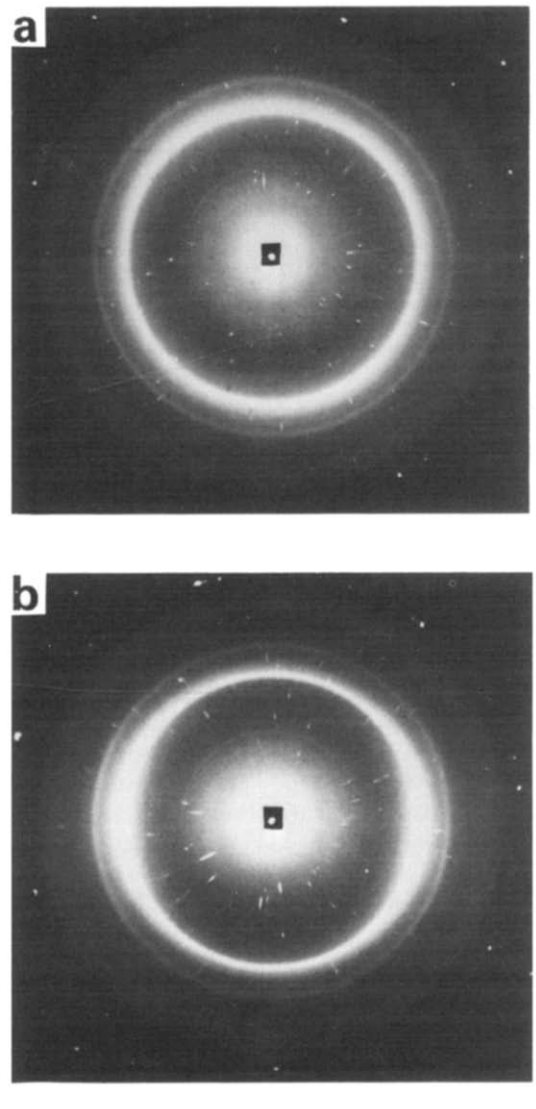


**Figure 9** Flat-plate diffraction photograph of a heat-pressed type A film (a). Photograph (b) was obtained from the same region after thermal cycling and resolidification

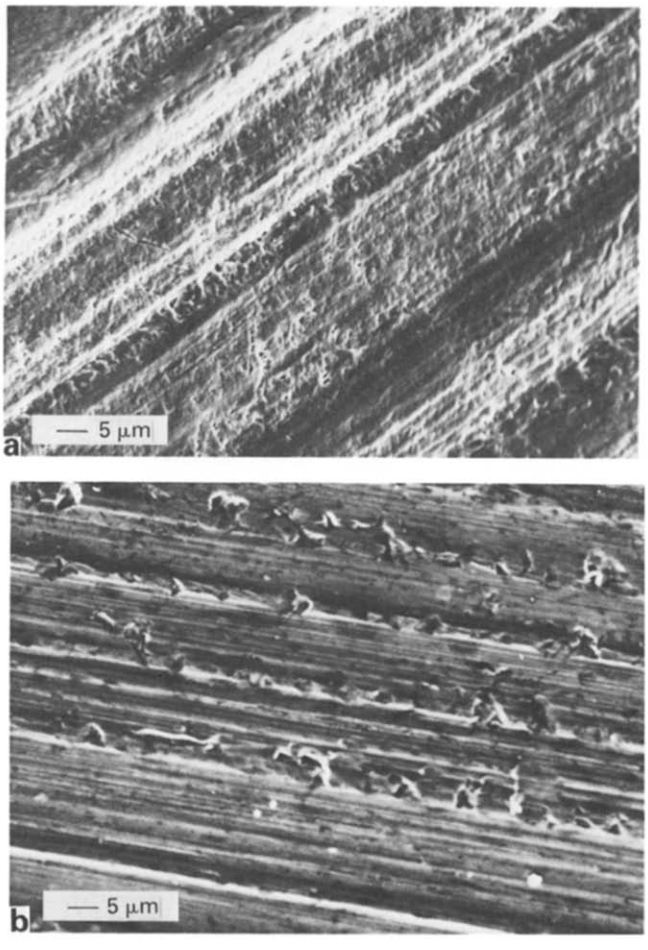


**Figure 10** Scanning electron micrographs of grooved surfaces on which the polymer was solidified: (a) corresponds to a Teflon surface and (b) corresponds to aluminium foil

aged samples could be explained by the formation of infusible crystals. In this particular context, the $E$ field would be viewed as an external influence which inhibits the chemical or physical mechanisms involved in thermal ageing of this mesophase. Also, a higher enthalpy of fusion in crystals formed under the influence of the field cannot be ruled out.

*Tables 3* and *4* contain data on orientation for samples solidified under an electric field. Exposure of the liquid-crystalline phase for 15 min to the electric field prior to solidification does not appear significantly to affect the molecular orientation of type A films. When the mesophase is exposed to the electric field for a period of 3 h prior to resolidification, molecular orientation improves slightly, but this could be the effect of mesophase ageing. On the other hand, significant results were obtained for samples that were melted and then resolidified under the field. The first fact that should be considered in understanding the field's effect is that orientation of low-molar-mass liquid crystals with low voltages does occur above some threshold value[7]. Judging from previous work referred to earlier, our experimental fields are above such thresholds. Given the presence of dipole moments nearly perpendicular to the director, one expects the liquid-crystal polymer studied to exhibit a negative dielectric anisotropy:

$$\varepsilon_{\parallel} - \varepsilon_{\perp} < 0$$

The ester bond dipole moment has a magnitude of approximately 1.8 D, inclined about 20–30° with respect to the C=O bond axes[35]. Consequently, the electric field would then tend to align the director axes normal to the electric field, resulting in a preferred planar orientation. However, pre-existing uniaxial chain orientation in the plane would be enhanced by the field since the electrical interaction rotates chains into this plane. Once in this plane, the pre-existing uniaxial field caused by surface or mechanical forces would cooperatively align other chains. This is an example of how an $E$ field could couple with a 'molecular field' to enhance uniaxial orientation even though the dielectric anisotropy is negative.

Most previous theoretical work on the interaction of $E$ fields and a mesophase is relevant to molecules of monomeric dimensions[36–38]. We currently lack a theoretical understanding of 'polymeric' effects in this interaction and also crystallization of nematic or smectic polymers under the influence of a field. Work done so far indicates that molecular shape and perhaps anisotropic polarizability are critical variables in the formation of polymeric mesophases. Other factors such as dipole–dipole interactions could play an important role in stabilizing or controlling the nematic vs. biaxial nematic or smectic nature of mesophases formed by polar chains. One indication of this is our finding of a large electrical polarization stored in poled films of the liquid-crystal polyester studied here[39]. The suggested biaxial nematic structure of a similar mesogenic polymer[40] could also be related to dipolar coupling.

We consider below interactions between the $E$ field and molecular dipoles in order to explore one interpretation

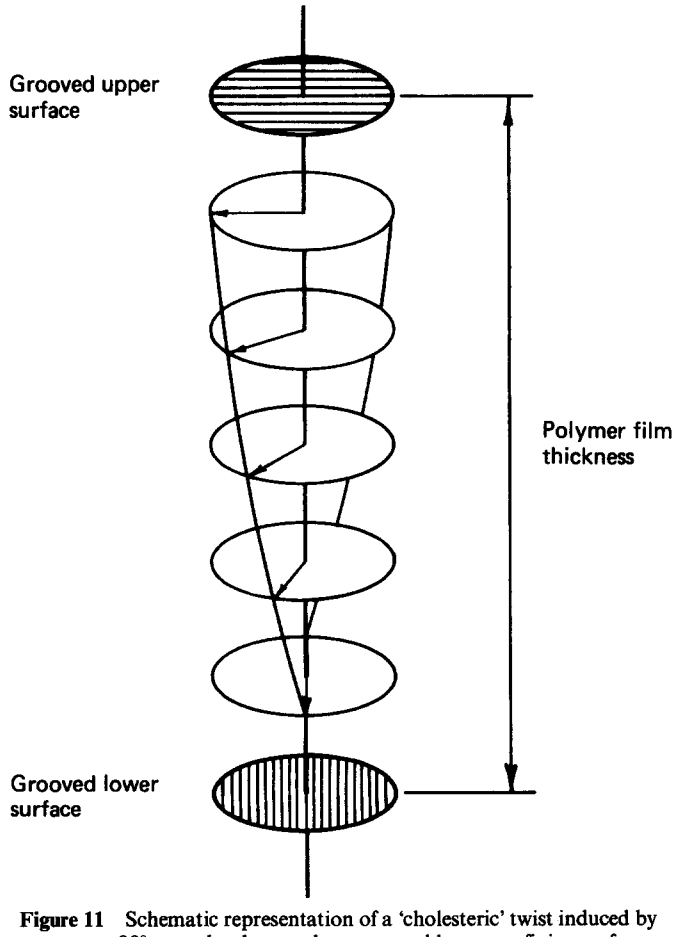


**Figure 11** Schematic representation of a 'cholesteric' twist induced by grooves at 90° to each other on the upper and lower confining surfaces. The arrow in the figure represents the director axis

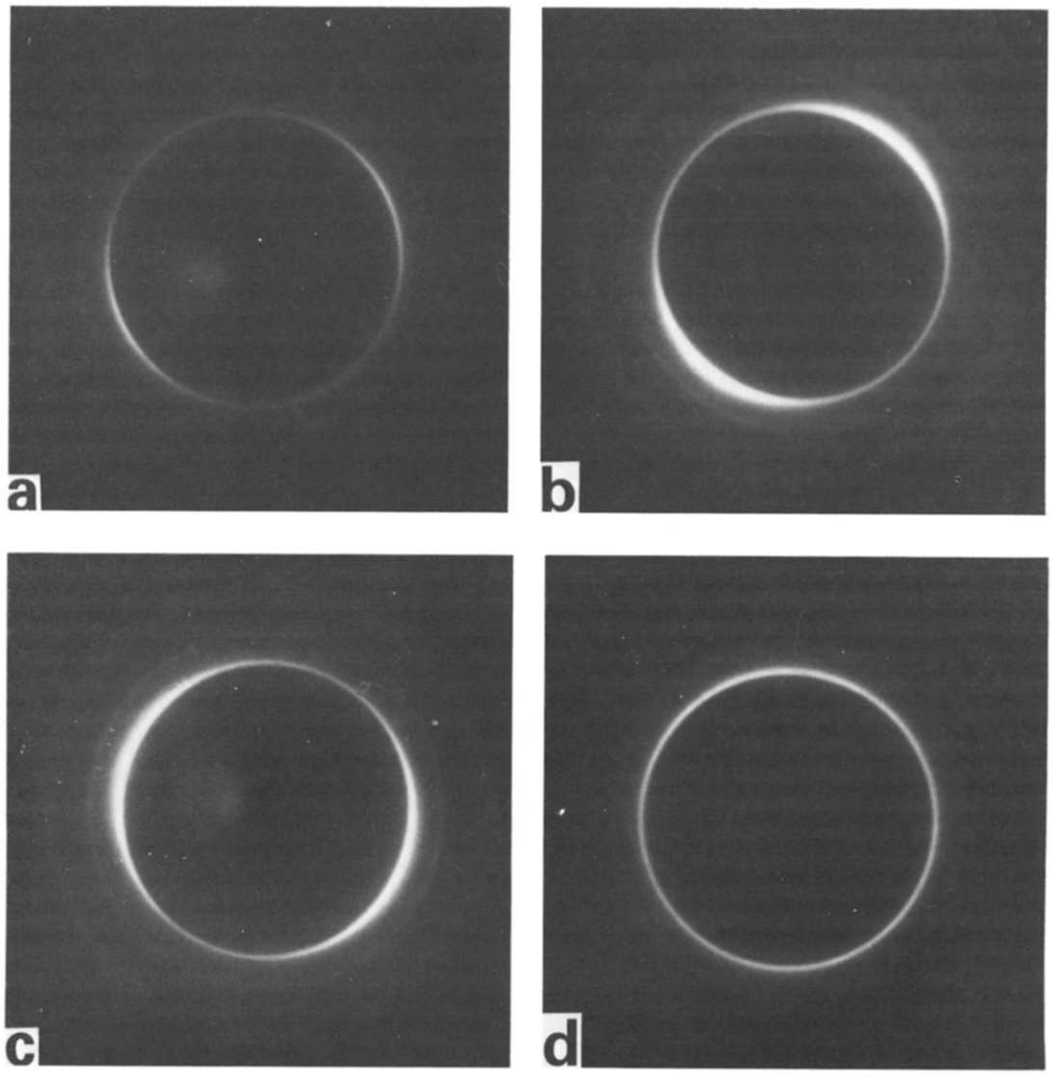


**Figure 12** Typical flat-plate diffraction photograph of heat-pressed type A film (a). The X-ray photograph (b) corresponds to the same region of the film after thermal cycling in contact with confining aluminium surfaces with parallel grooves. Photograph (c) corresponds to a heat-pressed type A film, and (d) to the same region after thermal cycling in contact with confining aluminium surfaces with grooves at 90° to each other

**Table 5** Average enthalpy values as measured by d.s.c.

| Sample | $\Delta H$ (J g$^{-1}$)[a] |
|---|---|
| Thermally cycled film, mesophase ageing in the range of 15–30 min | 6.85±1.70 |
| ~20 000 V cm$^{-1}$ $E$ field applied prior to solid-to-liquid crystal transition (15 min mesophase ageing) | 10.40±0.42 |

[a] Value±one standard deviation

**Table 6** Percentage distribution of total area under the d.s.c. endotherm in three different thermal ranges

| | Thermal ranges | | |
|---|---|---|---|
| Material | 240–295°C | 295–315°C | 315–345°C |
| Extruded pellets | 48.0 | 52.0 | 0 |
| Heat-pressed films | 43.4 | 34.1 | 22.5 |
| Mesophase-aged[a] | 45.4 | 25.8 | 28.8 |
| Field-crystallized[b] | 40.7 | 25.2 | 34.1 |

[a] Mesophase-aged for 20 min
[b] 20 000 V cm$^{-1}$ applied at room temperature

for the higher $\Delta H$ values in field-solidified samples. As a first-order approximation one may consider the interaction energy between two neighbouring dipole moments. The electric field $E$ at $x$ due to a dipole of moment $\mu$ positioned at $x_0$ is given by

$$E(x)=\frac{1}{4\pi\varepsilon_0}\frac{3\mathbf{n}(\boldsymbol{\mu}\cdot\mathbf{n})-\boldsymbol{\mu}}{|\mathbf{x}-\mathbf{x}_0|^3} \quad (2)$$

where $\varepsilon_0$ is the permittivity of vacuum, and where $\mathbf{n}$ is a unit vector in the direction from $\mathbf{x}_0$ to $\mathbf{x}$. Thus, the interaction energy $W_{12}$ between two dipoles is equal to

$$W_{12}=-\boldsymbol{\mu}\cdot\mathbf{E}=\frac{1}{4\pi\varepsilon_0}\frac{\boldsymbol{\mu}_1\cdot\boldsymbol{\mu}_2-3(\mathbf{n}\cdot\boldsymbol{\mu}_1)(\mathbf{n}\cdot\boldsymbol{\mu}_2)}{|\mathbf{x}_1-\mathbf{x}_2|^3} \quad (3)$$

As the mesophase solidifies under the influence of the external $E$ field, dipoles in neighbouring chain segments would tend to align head-to-tail as the field biases the moments into a common orientation. This coupling may or may not occur in the fluid phase. From equation (3), the interaction between two dipoles in a head-to-tail arrangement is equal to

$$W_{12}=\frac{1}{4\pi\varepsilon_0}\frac{-2\mu_1\mu_2}{|\mathbf{x}_1-\mathbf{x}_2|^3} \quad (4)$$

where $|\mathbf{x}_1 - \mathbf{x}_2|$ is a separation distance. For two ester dipoles with moment equal to 1.8 D at a separation distance of 5.9 Å, we calculate $W_{12}$ to be of the order of 0.45 kcal mol$^{-1}$. These calculations have used the unit cell parameters and density of PHB crystals and the results are fairly insensitive to small changes in $d$ spacings or degree of crystallinity. If a given fraction of the dipole moments, say 0.1–0.2, were coupled head-to-tail upon solidification of the mesophase under the influence of the field, $\Delta H$ could be enhanced by 1 or 2 J g$^{-1}$. Since X-ray scans of field-solidified samples did not reveal a significant increase in crystallinity, we suggest it is possible that higher $\Delta H$ values contain a 'contribution' from intermolecular interactions among field-aligned dipole moments. One must keep in mind, however, that a higher crystallinity could have developed in field-exposed samples during the d.s.c. scan. As discussed before, alignment of the mesogenic chains in the field (director perpendicular to the $E$ axis) could also inhibit the chemical or physical reorganization that leads to the formation of infusible crystals. This inhibition would then contribute to $\Delta H$ values being higher than those of thermal controls. Since the d.s.c. endotherm becomes very broad after mesophase ageing and resolidification, it is difficult to assess if an increase in melting point has occurred after exposure to the field. However, we integrated the d.s.c. endotherm over three different thermal ranges and results are presented in *Table 6*. Mesophase ageing for a brief period slightly raises the area in the highest thermal range with the effect being more pronounced in field-solidified samples. These observations are consistent with earlier discussions. The broad endotherm indicates a complex solid-state microstructure and there are probably different kinds of crystals in terms of size and defect content. Both mesophase ageing and field solidification could produce more of the higher-melting crystals or higher enthalpies of fusion.

As pointed out earlier, we observe field-induced orientation after 15 min in the mesophase only when the electrical exposure begins in the solid state at room temperature. This observation suggests a strong orientational cooperativity when the solid-to-mesophase transition occurs in an electrically poled state. Polarization due to dipolar orientation in the field will occur gradually as the solid is heated and molecular motions intensify. During the broad melting transition, poled solid nuclei which contain segments from several chains could contribute to a more effective cooperative alignment. Dipolar correlations within such nuclei would give rise to a moment which senses a strong torque due to the external field. The ability of dipoles within poled regions or poled nuclei to respond in unison to the field could be related to the 'biaxial' nature of these nematics. In general, one may suggest that molecular alignment in the field occurs more readily when solid poled nuclei are still dispersed in the mesophase.

An important factor which could interfere with dielectric alignment is the electrohydrodynamic flows known to occur in liquid crystals under the influence of $E$ fields[10,11]. These flows and their distinct patterns have been observed in liquid-crystal polymers[18,22–24], including copolyesters similar to the one used in this work[18]. The observations range from Williams domains to turbulent flows at high d.c. voltages, and tend to appear very slowly (within a few hours in some cases). Electrohydrodynamic instabilities have been associated with anisotropic conductivity, leading to space-charge segregation and local fields normal to the applied field. Based on the discussion above, electrohydrodynamic effects are possibly interfering with dielectric alignment in our samples, specially in long exposures. However, such flows do not preclude some dielectric alignment as the mesophase solidifies. We do not know at the present time if the enhanced orientation observed when films are melted and resolidified under the field is related in any way to the 'absence' of electrohydrodynamic phenomena under those conditions. The poled state of the film at the time of melting could include the presence of a space charge and thus may interfere with electrohydrodynamic effects. This is a possibility we will consider in future work.

## CONCLUSIONS

The solid-state structure of liquid-crystal polymers can be affected by exposure of the fluid to an external electric field and also by thermal ageing of the mesophase. The original solid-state structure prior to melting and the topography of the surface on which resolidification occurs are also important structure-determining factors. Preferred backbone orientation can be detected in resolidified films even after the mesophase is thermally aged for periods of 3 h. Electric fields enhance molecular orientation when the exposure to the field begins below the solid-to-mesophase transition. The electric field is also effective in inducing preferred orientation when coupled to a pre-existing molecular field in a favourable dielectric alignment. These observations as well as a higher enthalpy for the solid-to-mesophase transition in samples solidified in electric fields could be related to dipole–dipole coupling in poled structures. This coupling could be the result of a biaxial nematic structure in these polymers.

## ACKNOWLEDGEMENTS

This work has been supported by the National Science Foundation Grant NSF-DMR 83-16981, obtained through the Materials Research Laboratory of the University of Illinois. The authors also acknowledge Dr J. Jackson from Tennessee Eastman for supplying us with the experimental material and the use of facilities at the University of Illinois Center for Electron Microscopy.

## APPENDIX

The plot in *Figure 8* was generated using the following model. The total intensity contained in the Debye ring, $I_T$, is divided into two separate contributions, an unoriented component, $I_{un}$, and an oriented component, $I_{or}$:

$$I_{or} = \alpha I_T$$

$$I_{un} = (100 - \alpha) I_T$$

where $\alpha$ is the percentage orientation for a given X-ray path through the sample. $I_{un}$ is decomposed into 24 equal constituents, $x$, distributed uniformly around the ring (24 constituents, since this was the number of densitometer scans obtained around the ring). $I_{or}$ is decomposed into two equal constituents (two constituents, since it is

assumed that the ring decomposes into two arcs), superimposed on a fraction of the unoriented component, $y$:

$$x = I_{un}/24$$

$$y = I_{un}/24 + I_{or}/2$$

Using this model, a mean intensity, $\bar{x}_I$, and a standard deviation, $\sigma_I$, are calculated for various values of $\alpha$:

$$\bar{x}_I = \frac{22x + 2y}{24}$$

$$\sigma_I = \left( \frac{22x^2 + 2y^2 - (22x + 2y)^2/24}{23} \right)^{\frac{1}{2}}$$

The ratio of $\sigma_I/\bar{x}_I$ was calculated for values of $\alpha$ in the range 0–100% (see *Figure 8*). Experimental values of $\sigma_I/\bar{x}_I$ obtained from densitometer scans were compared with the calculated values in *Figure 8* in order to assess changes in degree of orientation.

## REFERENCES


1 Shibaev, V. P., Kostromin, S. G., Plate, N. A., Ivanov, S. A., Vetrov, V. Y. and Yakovlev, I. A. *Polymer* 1983, **24** (*Commun*), 364
2 Chapoy. L. L., Biddle, D., Halstrom, J., Kovacs, K., Brunfeldt, K., Qasim, M. A. and Christen, T. *Macromolecules* 1983, **16**, 181
3 Biddle, D. and Chapoy, L. L. *Macromolecules* 1984, **17**, 1751
4 Flory, P. J. *Proc. R. Soc. Lond. A* 1956, **234**, 73
5 Flory, P. J. and Abe, A. *Macromolecules* 1978, **11**, 1119
6 Flory, P. J. *Macromolecules* 1978, **11**, 1141
7 Helfrich, W. *Mol. Cryst. Liq. Cryst.* 1973, **21**, 187
8 Carr, E. F. *Mol. Cryst. Liq. Cryst.* 1969, **7**, 253
9 Williams, R. J. *J. Chem. Phys.* 1963, **39**, 384
10 Penz, P. A. *Phys. Rev. Lett.* 1970, **24**, 1405
11 Orsay Liquid Crystal Group, *Phys. Lett.* 1972, **39A**, 181
12 Penz, P. A. and Ford, G. W. *Phys. Rev. A* 1972, **6**, 414
13 Carroll, T. O. *J. Appl. Phys.* 1972, **43**, 1342
14 Finkelmann, H., Naegele, D. and Ringsdorf, H. *Makromol. Chem.* 1979, **180**, 803
15 Talroze, R. V., Kostromin, S. G., Shibaev, V. P., Plate, N. A., Kreese, H., Sauer, K. and Demus, D. *Makromol. Chem., Rapid Commun.* 1981, **2**, 305
16 Ringsdorf, H. and Zentel, R. *Makromol. Chem.* 1982, **183**, 1245
17 Ringsdorf, H. and Schmidt, H. *Makromol. Chem.* 1984, **185**, 1327
18 Krigbaum, W. R., Lader, H. S. and Ciferri, A. *Macromolecules* 1980, **13**, 554
19 Krigbaum, W. R., Grantham, C. E. and Toriumi, H. *Macromolecules* 1982, **15**, 592
20 Gilli, J. M., Schmidt, H. W., Pinton, J. F., Sixou, P., Thomas, O., Kharas, G. and Blumstein, A. *Mol. Cryst. Liq. Cryst. Lett.* 1984, **102**, 49
21 Gilli, J. M., Pinton, J. F., Sixou, P., Blumstein, A. and Thomas, O. *Mol. Cryst. Liq. Cryst. Lett.* 1985, **1**, 123
22 Minami, N., Aikawa, Y. and Sukigara, M. *Mol. Cryst. Liq. Cryst. Lett.* 1978, **41**, 189
23 Blumstein, A., Schmidt, H. W., Thomas, O., Kharas, G. R. and Blumstein, R. B. *Mol. Cryst. Liq. Cryst. Lett.* 1984, **92**, 271
24 Gilli, J. M., Ten Bosch, A., Pinton, J. F., Sixou, P., Blumstein, A. and Blumstein, R. B. *Mol. Cryst. Liq. Cryst.* 1984, **105**, 375
25 Jackson, W. J., Jr and Kuhfuss, H. F. *J. Polym. Sci., Polym. Chem. Edn.* 1976, **14**, 2043
26 Economy, J., Storm, R. S., Matkovich, V. I., Cottis, S. G. and Nowak, B. E. *J. Polym. Sci., Polym. Chem. Edn.* 1976, **14**, 2207
27 McFarlane, F. E., Nicely, V. A. and Davis, T. G. 'Contemporty Topics in Polymer Science' (Eds. E. M. Pierce and J. R. Schaefgen), Plenum Press, New York, 1977, Vol. 2
28 Zachariades, A. E., Economy, J. and Logan, J. A. *J. Appl. Polym. Sci.* 1982, **27**, 2009
29 Meesiri, W., Menczel, S., Gaur, U. and Wunderlich, B. *J. Polym. Sci., Polym. Phys. Edn.* 1982, **20**, 719
30 Blackwell, J., Lieser, G. and Gutierrez, G. A. *Macromolecules* 1983, **16**, 1418
31 Challa, G., Hermans, P. H. and Weidinger, A. *Makromol. Chem.* 1962, **56**, 169
32 Lenz, R. W., Jin, J. and Feichtinger, K. A. *Polymer* 1983, **24**, 327
33 Berreman, D. W. *Mol. Cryst. Liq. Cryst.* 1973, **23**, 215
34 Schadt, M. and Helfrich, W. *Appl. Phys. Lett.* 1971, **18**, 127
35 Flory, P. J. 'Statistical Mechanics of Chain Molecules', John Wiley and Sons, New York, 1969, p. 267
36 Helfrich, W. *J. Chem. Phys.* 1969, **51**, 4092
37 Meyer, R. *Phys. Rev. Lett.* 1969, **22**, 918
38 Gruler, H. and Meier, G. *Mol. Cryst. Liq. Cryst.* 1972, **16**, 299
39 Stupp, S. I., Martin, P. G. and Landreth, B. M. submitted for publication
40 Mitchell, G. R. and Windle, A. *Polymer* 1982, **23**, 1269